

STRUCTURAL RELIABILITY OF PRE-STRESSED CONCRETE CONTAINMENTS

Nawal K Prinja¹, Azeezat Ogunbadejo², Jonathan Sadeghi³ and Edoardo Patelli⁴

¹Technical Director, Clean Energy, AMEC Foster Wheeler, Booths Park, Knutsford, Cheshire WA16 8QZ, UK

²MSc student, School of Eng., University of Aberdeen

³PhD student, Institute for Risk and Uncertainty, University of Liverpool

⁴Lecturer, Institute for Risk and Uncertainty, University of Liverpool

E-mail of corresponding author: nawal.prinja@amecfw.com

ABSTRACT

This paper presents probabilistic analysis of structural capacity of pre-stressed concrete containments subjected to internal pressure. The conventional design methods for containments are based on allowable stress codes which ensure certain factor of safety between expected load and expected structural strength. Such an approach may give different values of structural reliability in different situations. In recent years, two international round robin exercises have been conducted aimed at predicting the capacity of lined and unlined pre-stressed concrete containments used in nuclear industry. These exercises involved experimental testing and numerical analysis of the models. The first exercise involved ¼ scale steel-lined Pre-stressed Concrete Containment Vessel (PCCV) which was tested at Sandia National Laboratories (SNL) in USA. The second used an unlined containment being tested by the Bhabha Atomic Research Centre (BARC), Tarapur, India. These studies are essentially deterministic studies that have helped validate the analysis methodology and modelling techniques that can be used to predict pre-stressed concrete containment capacity and failure modes. The paper uses these two examples to apply structural reliability method to estimate the probability of failure of the containment.

The two international round robin exercises have already established the ultimate structural collapse mode of the containments under internal pressure loading which indicate that the failure takes place in the general field of the containment wall around mid-height and away from any major structural discontinuities like the penetrations. This is because robust design procedures have been used to avoid structural failure at discontinuities by providing adequate compensation. Based on these experimental studies and the attendant numerical analyses a failure function is presented that assumes first yielding in the hoop direction at mid-height of the cylinder wall. A failure function equating the free-field membrane hoop stress to the hoop strength as a function of cross-sectional area (per unit height) and yield stresses of concrete, rebar, liner plate and tendons is developed.

First Order Reliability Method (FORM) is applied to predict probability of failure of the containments. Probability of failure vs internal pressure is presented for both types of containments. The paper presents a simple method to establish structural reliability of a pre-stressed concrete containment which can be useful for probabilistic safety assessment when considering extreme events that lead to over-pressurisation of the containment. The FORM approach was validated by comparison to the results of analogous calculations using Subset Simulation and Importance Sampling techniques for Monte Carlo simulation. It was found that at high pressures the Advanced FORM approach yields a good approximation to the true probability of failure.

The sensitivity of the probability of failure to the assumed coefficients of variation of properties of the containment was studied using the Sobol and Total Effects Indices. At design pressure it was found that the coefficients of variation of the tendon yield and tendon area are the most important parameters followed by the applied pressure and containment radius. At higher pressures it was found that the

coefficients of variation of the applied pressure and containment radius are the most important parameters. The variability of the probability of failure is decreased at higher pressures, but the coefficients of variation still play an important role.

KEYWORDS

Concrete containment, structural reliability, containment capacity, probabilistic safety assessment, fragility, sensitivity analysis, coefficient of variation.

INTRODUCTION

A pre-stressed concrete containment is an important safety related structure as it acts as one of the final barriers to radioactive release. These structures are normally designed in accordance with the allowable stress codes to sustain the specified loading conditions. However, the compliance with the industry standard allowable stress codes does not give any reliable indication of the probability of failure (P_f) if the containment is over-pressurised under postulated beyond design basis events. In the past few years, two international round robin exercises have been conducted which have provided valuable test data related to failure under over-pressurisation. The first exercise involved the numerical analysis of the $\frac{1}{4}$ scale steel-lined Pre-stressed Concrete Containment Vessel (PCCV) with design pressure (P_d) of 0.39MPa which was tested at Sandia National Laboratories (SNL) in USA and has been analysed by Prinja and Shepherd (2003). The second exercise involved the unlined Bhabha Atomic Research Centre (BARC) Containment test model (BARCOM) with P_d of 0.1413 MPa that is being tested by the BARC in Tarapur, India and has been analysed by Kamatam and Prinja (2011). These studies are essentially deterministic studies that have helped validate the analysis methodology and modelling techniques that can be used to predict pre-stressed concrete containment capacity and failure modes. Such deterministic analytical and experimental studies have helped to establish the mode of failure but do not give any indication of P_f . Furthermore, the conventional allowable stress codes used to design such containments also do not provide P_f information. The aim of this paper is to present a simple method to establish structural reliability of a pre-stressed concrete containment which can be useful for probabilistic safety assessment when considering over-pressurisation under extreme events.

The method used to perform the analysis was Advanced FORM, a computationally efficient approximate method. In addition, Sensitivity Analysis was used in order to justify some arbitrary parameters used in the structural reliability analysis. Sensitivity Analysis is the process of attributing the uncertainty in the output of a mathematical model to the different sources of uncertainty in its inputs. In this paper we determine the sensitivity of the probability of failure of a concrete containment vessel to the assumed coefficients of variation of input parameters to the structural reliability analysis. These input parameters are physical properties of the containment. Before the sensitivity analysis was completed, the FORM method was validated for the containment at the design pressure and at 5.4 times the design pressure to provide an indication of the credibility of the FORM. This calculation was performed by comparing the results from the FORM to the true value of the probability of failure obtained from Subset Simulation and Importance Sampling as it was found that the failure probability was too small to be evaluated in a short time using standard Monte Carlo simulation. Once this was completed the parameters whose variance had the greatest contribution to the variance of the output were determined using the Sobol and Total Effects indices, and the effect on P_f of varying these parameters was considered in greater detail.

FAILURE MODE

Both SNL and BARCOM tests have shown that the collapse of the containment structure subjected to internal pressure is not expected to occur soon after the design pressure is exceeded. There is no 'cliff edge' but a gradual progressive damage of the containment structure under over-pressurisation which

indicates safety margin against collapse. The structure may suffer local failures leading to functional failure well before the ultimate structural collapse. The experiments and the attendant numerical analyses have established the ultimate structural collapse mode of the containments under internal pressure loading which indicates that the failure takes place in the general field of the containment wall around mid-height and away from any major structural discontinuities like the penetrations. This is because robust design procedures have been used that provide adequate compensation and local strengthening to avoid structural failure at discontinuities. Based on these experimental studies and the attendant numerical analyses a failure function is presented that assumes first yielding in the hoop direction at mid-height of the cylinder wall.

In the case of the SNL model shown in Figure 1, the failure location at applied pressure (P) of 3.65 Pd was accurately predicted by the computational model at mid-height of the cylinder in the general area away from the buttress and main penetrations. The BARCOM model is also predicted to fail at mid-height of the cylinder wall as indicated in the deformed shape shown in Figure 2.

Load-deflection curve obtained from the test is compared against that predicted by analysis for the SNL model in Figure 3 at location 14 near the failure location. Note that in the test the internal pressure is released soon after the break but in the analysis the pressure is maintained. The SNL model failed at P/Pd=3.65 in test and was predicted to fail at P/Pd=3.35 in the analysis.

FAILURE FUNCTION

Failure of a containment structure is dictated by the strain levels experienced by the tendons, rebars and the liner following the tensile cracking of the concrete. The first membrane yield is expected to occur in the hoop direction in the cylinder wall. If the failure state is defined as the tensile cracking of the concrete and yielding of the tendons, rebars and the liner, then the internal pressure at a specific deformed shape is given by:

$$P = \frac{1}{R}(A_s * F_s + A_c * F_c + A_l * F_l + A_t * F_t) \quad (1)$$

Where A_s , A_c , A_l , A_t are cross-sectional areas of the rebar steel, concrete, liner plate and tendons respectively given as area per unit height of the cylinder wall. F_s , F_l and F_t are yield stress of rebar steel, liner plate and tendons respectively and F_c is the tensile strength of the concrete. R is the mid-radius of the cylinder wall.

The failure function 'g' can be written as:

$$g = PR - (A_s * F_s + A_c * F_c + A_l * F_l + A_t * F_t) \quad (2)$$

FORM Analysis

If Z is a function of many basic variables then $Z = g(x_1, x_2, \dots, x_n) = 0$ can be written using Taylor series as:

$$Z = g(x_1^*, x_2^*, \dots, x_n^*) + \sum_{i=1}^{i=n} (x_i - x_i^*) g'_i(x^*) + \dots \quad (3)$$

where $g'_i(x^*)$ is derivative $\frac{\partial g}{\partial x_i}$ evaluated at $x_i = x_i^*$

$$Z = k_0 + \sum_{i=1}^{i=n} k_i x_i \quad (4)$$

The mean μ_Z and standard deviation σ_Z of Z are given as:

$$\mu_Z = k_0 + \sum_{i=1}^{i=n} k_i m_i \quad (5)$$

$$\sigma_Z = \left[\sum_{i=1}^{i=n} k_i^2 \sigma_i^2 \right]^{\frac{1}{2}} \quad (6)$$

The reliability index, β is given by

$$\beta = \frac{\mu_Z}{\sigma_Z} \quad \text{with probability of failure, } P_f = \phi(-\beta) \text{ and reliability, } R = 1 - \phi(-\beta) \quad (7)$$

where ϕ is the standardised cumulative normal distribution.

In structural reliability, eqn (2) can also be written in terms of load (L) and strength (S) terms as follows:

$$Z = g(x_1, x_2, \dots, x_n) = S - L \quad (8)$$

where $S = (A_s * F_s + A_c * F_c + A_l * F_l + A_t * F_t)$ and $L = PR$

If μ_S and μ_L are mean values and V_S and V_L are coefficient of variation (CoV) of the strength and the load terms (S and L) respectively, then the reliability index, β can be written in terms of Central Factor of Safety (η) defined as the ratio of the mean values of S and L terms ($\eta = \mu_S / \mu_L$) :

$$\beta = \frac{(\mu_S - \mu_L)}{\sqrt{(\sigma_S^2 + \sigma_L^2)}} = \frac{(\frac{\mu_S}{\mu_L} - 1)}{\sqrt{(\frac{\sigma_S}{\mu_L})^2 + (\frac{\sigma_L}{\mu_L})^2}} = \frac{(\frac{\mu_S}{\mu_L} - 1)}{\sqrt{(\frac{\sigma_S}{\mu_S})^2 (\frac{\mu_S}{\mu_L})^2 + (\frac{\sigma_L}{\mu_L})^2}} \quad (9)$$

$$\beta = \frac{(\eta - 1)}{\sqrt{(V_S^2 \eta^2 + V_L^2)}} \quad (10)$$

The above equation has been used to obtain P_f for various values of the Central Factor of Safety assuming that CoV of both load and strength terms are equal. Figure 4 shows the P_f vs η plots for CoV of 0.1 and 0.2. It can be seen that when $V_S = V_L$, the probability of failure is 50% when the load term equals the strength term.

Advanced FORM Analysis

The failure function of the containment structure given in eqn (2) has ten variables. When all ten variables are used, the failure function becomes nonlinear and advanced FORM analysis is used following the iterative algorithm recommend by Rackwitz (1976):-

1. Guess an initial value of β typically starting with $\beta = 3$
2. Set $x_i^* = \mu_i$ for all i. All variables set to their respective mean value μ at the start.

3. Compute partial derivative of $\frac{\partial g}{\partial x_i}$ also known as a_i for all i at $x = x^*$
4. Compute Sensitivity factors, $\alpha_i = \frac{a_i \sigma_i}{\sqrt{\sum_{j=1}^{j=n} (a_j \sigma_j)^2}}$
5. Compute new x^* values using $x_i^* = \mu_i - (\alpha_i \beta \sigma_i)$
6. Repeat step 3 to 5 to get stable values of all x^*
7. Evaluate $z = g(x_1^*, x_2^*, \dots, x_n^*)$
8. Evaluate $\frac{dz}{d\beta}$ using $\frac{dz}{d\beta} = \sum -a_i \alpha_i \sigma_i$
9. $\beta_{new} = \beta_{old} - Z_n / \frac{dz}{d\beta}$
10. Compute modified design values $x_i^* = \mu_i - (\alpha_i \beta \sigma_i)$
11. Repeat steps 3 to 11 till stable value of β is achieved.
12. Calculate probability of failure, $P_f = \varphi(-\beta)$

PROBABILITY OF FAILURE CALCULATIONS

The cross-sectional area properties were obtained from the geometric data as follows:-

Steel rebar area/unit height, $A_s = n_s * \pi * r_s^2 / h_s$

Where n_s = number of steel rebars through wall thickness
 r_s is radius of steel rebar and h_s is the vertical spacing.

Liner area/unit height, $A_l = \text{thickness of the plate} \times 1$

Tendon area/unit height, $A_t = n_t * \pi * r_t^2 / h_t$

Where n_t = number of tendons through wall thickness. r_t is tendon radius and h_t is tendon vertical spacing.

Concrete area/unit height, $A_c = ((r_o - r_i) - (A_l + A_s + A_t))$

r_o and r_i are outer and inner radii of the wall and mid-radius of the wall, $R = (r_o + r_i)/2$.

SNL Containment Data

In the SNL model, each tendon is built from 3 wires of 13.7mm diameter so and there were 90 hoop tendons in the wall height of 10750mm giving tendon vertical spacing, $h_t = 119.4\text{mm}$.

With $n_t = 3$ and $r_t = 6.85\text{mm}$

$$A_t = (3 * 3.14 * 6.85 * 6.85) / 119.4 = 3.70 \text{ mm}^2 / \text{mm}$$

There are two hoop rebars (inner and outer) of 22.2mm dia which are vertically spaced at 113mm interval. With $n_s = 2$ and $r_s = 11.1\text{mm}$

$$A_s = (2 * 3.142 * 11.1 * 11.1) / 113 = 6.85 \text{ mm}^2 / \text{mm}$$

$$A_l = \text{thickness of the plate} \times 1 = 1.6 \text{ mm}^2 / \text{mm}$$

$$A_c = 312.85 \text{ mm}^2 / \text{mm}$$

Where $r_o = 5700\text{mm}$, $r_i = 5375\text{mm}$ and $R = 5537.5\text{mm}$

BARCOM Containment Data

The BARCOM model has no liner so $A_l=0$. In the area of failure there are two steel rebars of 12mm dia used as hoop reinforcement through the thickness of the wall at intervals of 200mm. Therefore,
 $A_s = (2 \times 3.14 \times 6 \times 6) / 200 = 1.1304 \text{ mm}^2/\text{mm}$

One 24mm dia hoop tendon (horizontal cable) is placed at vertical interval of 110mm giving
 $A_t = 4.11 \text{ mm}^2/\text{mm}$. The wall is 188mm thick and goes from elevation level -2.25m to +9.025m giving wall height of 11275mm.

$r_o = 6376\text{mm}$, $r_i = 6188\text{mm}$ and $R = 6282\text{mm}$.
Therefore, $A_c = 182.76\text{mm}^2/\text{mm}$.

The geometric data is summarised in table 1.

The applied internal pressure (P) is increased from 0 MPa till probability of failure (P_f) of 1.0 is achieved.

Statistical Data for Material and Geometry

In structural reliability analysis for concrete containment capacities, tensile strength of two different types of materials need to be considered: concrete and steel. Concrete behaves like a brittle material whereas steel components like the tendons, rebars and liner plate will exhibit plastic behaviour when loaded beyond their yield stress. In case of concrete, variability in strength can be traced to two fundamentally different sources: variability in the properties of the concrete mixture and ingredients and variability in the way the strength is tested and measured. Similarly variability in yield strength of a given steel varies due to variation in chemistry, heat treatment and mechanical processing. Typically, it is the compressive strength concrete which is specified and measured. The tensile strength of concrete is taken to be about 10% of its compressive strength at room temperature. At higher temperatures, the strength tends to decrease and any loss in the tensile strength is proportional to the corresponding loss in the compressive strength.

Variability in geometric dimensions of engineered components depends on the manufacturing process and the specified tolerances. Usually tolerances in manufacturing processes are tight and tend to follow normal distribution.

In this example, all material, geometric and loading parameters are assumed to have CoV of 0.2 with normal distribution. In practice, the CoV in yield strength of steel components could be less than 0.1 and the CoV of geometric dimensions could be even lower.

Mean values and coefficient of variation used for strength and loading variables are given in table 2.

Results

Figure 5 presents P/P_d vs P_f curves for both SNL and BARCOM models obtained by using the advanced FORM analysis. Two curves for each model are presented. One in which all ten variables were considered and the other in which the concrete was assumed to be totally damaged due to previous testing and was assigned zero strength. Similar sensitivity exercises can be conducted to study the influence of variation in material, loading and geometric parameters. Failure curves of the kind depicted in Figure 5 can be used to define the fragility of concrete containments under over-pressure.

DISCUSSION AND CONCLUSIONS

The available test data and the FEA results (Kamatam & Prinja (2011) and Prinja & Shepherd (2003)) showed that the structural response of the pressurised PCCV is indicated by progressive damage in three stages. The first stage up to the design pressure ($P/P_d=1$) is predominantly elastic response and can be predicted with very good accuracy. The second stage involving inelastic response with extensive concrete cracking with local yielding or rupture may lead to loss of functionality (leakage) or breach of pressure boundary. The third stage involves gross deformation leading to the structural collapse. The P_f of this gross structural collapse depends on the amount of steel and concrete used in the design as given in equation 1. The strength terms (given by area x yield stress) for rebar, liner, tendon and concrete are compared in Table 3 for the SNL and BARCOM models along with the design load term (given by P_d x mid-radius of the wall). It can be seen that whilst the overall strength of the two containment models is almost similar, the load term of the BARCOM model is only 40% of the SNL model. The strength/load ratio (γ) for the SNL is 5.4 but for the BARCOM model it is 9.7 so overall the BARCOM model is nearly twice as strong as the SNL model. This is reflected in the P_f vs P/P_d curves presented in Fig 5. In case of the SNL model, the load term equals the strength term when $P=5.4P_d$ but for the BARCOM model it is when $P=9.7P_d$. Therefore, the P_f for SNL is 50% when $P=5.4P_d$ but in the test, the SNL model failed catastrophically at $P=3.65P_d$. Catastrophic failure at pressure lower than $5.4P_d$ could be because of extensive damage to the concrete and the liner due to earlier testing. If similar trend is to be followed then the BARCOM model has to be pressurised beyond $9.7P_d$. Such pressurisation in a test may not be easily achieved due to problems with localised failures and leakage.

Table 1 Summary of geometric data for the SNL and BARCOM models

Geometric Data	SNL	BARCOM
Outside radius of the wall, r_o (mm)	5700	6376
Inner radius of the wall, r_i (mm)	5375	6188
Wall thickness (mm)	325	188
Wall height (mm)	10750	11275
Mid-radius, R (mm)	5537.5	6282
No. of tendons through wall, n_t	3	1
Tendon vertical spacing, h_t (mm)	119.4	110
Tendon radius, r_t (mm)	6.85	12
Tendon area, A_t (mm ² /mm)	3.70	4.11
No. of rebars through wall, n_s	2	2
Rebar vertical spacing, h_s (mm)	113	200
Rebar radius, r_s (mm)	11.1	6
Steel rebar area, A_s (mm ² /mm)	6.85	1.13
Liner plate thickness (mm)	1.6	0
Liner area, A_l (mm ² /mm)	1.6	0
Concrete area, A_c (mm ² /mm)	312.85	182.76

Table 2 Mean values of parameters used for SNL and BARCOM containments

Load and Strength Data	Mean Values (μ)		BARCOM/SNL	CoV
	SNL	BARCOM		
Concrete tensile strength, F_c	4.4	3.018	69%	0.2
Liner yield, F_l	382	0		0.2
Rebar Yield, F_s	465	415	89%	0.2
Tendon yield, F_t	1740	1848	106%	0.2
Design Pressure, P_d	0.39	0.1413		0.2
Radius, R	5537.5	6282.0	113%	0.2
Concrete Area, A_c	312.85	182.76	58%	0.2
Liner area, A_l	1.6	0	0%	0.2
Rebar Area, A_s	6.85	1.13	17%	0.2
Tendon area, A_t	3.70	4.11	111%	0.2

Table 3 Relative Strength and Load Terms for SNL and BARCOM containments

Strength Term	SNL	BARCOM	BARCOM/SNL
Rebar ($A_s \times F_s$)	3184.1	469.1	0.1
Liner ($A_l \times F_l$)	611.2	0.0	0.0
Tendon ($A_t \times F_t$)	6439.0	7596.3	1.2
Concrete ($A_c \times F_c$)	1376.5	551.6	0.4
Total Strength term, S	11610.8	8617.0	0.7
Design Load Term ($L = P_d \times R$)	2159.6	887.6	0.4
Strength/Load Ratio (γ)	5.4	9.7	1.8

SIMPLIFIED METHOD FOR STRUCTURAL RELIABILITY OF CONCRETE CONTAINMENTS

Assuming that the structural collapse of a containment occurs at the mid-height of the wall, the P_f of the containment can be estimated using the simplified procedure presented in Fig 6. All that is required is mean values of the five geometric (A_s , A_c , A_l , A_t and R) and four material (F_s , F_l , F_t and F_c) variables to establish the strength/design load ratio (γ). The $P_f = 0.5$ when the applied pressure, $P = \gamma P_d$. P_f at other pressures can be obtained by using either the simple FORM (eqn 10) or advanced FORM for which CoV values for all ten variables are required.

VALIDATION OF ADVANCED FORM

As advanced FORM is an approximate method, the method will be validated by comparing the obtained P_f from FORM to the equivalent P_f from Monte Carlo sampling. As the failure probability when the mean pressure is equal to the design pressure is small, the variance of the estimator of P_f is large. This is because it is difficult to obtain enough samples to sufficiently reduce the variance in a reasonable computational time. Therefore the variance reduction strategies of Subset Simulation and Importance Sampling were used to obtain P_f , and these were compared with the result from Advanced FORM. For both of these algorithms the implementation in the generalized uncertainty quantification software OpenCOSSAN was used (Patelli, 2014 and Patelli, 2016).

P_f was also calculated with an increased value of the mean value of P , $P = 5.4 P_d$, using the advanced FORM and compared to the result from standard Monte Carlo simulation. Standard Monte Carlo simulation was applicable for this calculation because variance reduction strategies are not required when P_f is large.

The input parameter values assumed in this analysis were taken from the Sandia National Laboratories tests (Table 2), and in order to make a fair comparison it was assumed that the random variables were normally distributed.

IMPORTANCE SAMPLING

The Monte Carlo estimator of failure probability is given by

$$P_f = \int I_f(x) f_X(x) dx = \frac{1}{n} \sum_{i=1}^n I_f(x_i), \quad (11)$$

where x_i are samples drawn from $f_X(x)$, the probability density function of the random variables, and $I_f(x)$ is the indicator function for the failure domain (i.e. $I_f(x)$ is non-zero only in the failure region given by $g(x) \geq 0$ from Equation 2). In Importance Sampling samples are drawn from a distribution with a higher density in the failure region, thereby reducing the variance of the estimator. Therefore the estimator is written as

$$P_f = \int \frac{I_f(x) f_X(x)}{h(x)} h(x) dx = \frac{1}{n} \sum_{i=1}^n \frac{I_f(x_i) f_X(x_i)}{h(x_i)}, \quad (12)$$

where x_i are drawn from $h(x)$. By finding the design point with an approximate method an appropriate $h(x)$ can be chosen. A more complete discussion of the technique is given in (Schuëller & Stix, 1987).

SUBSET SIMULATION

Subset simulation aims to calculate P_f by decomposing the space of the random variables into several intermediate failure events with decreasing failure probability. The conditional probabilities for the intermediate failure regions can then be used to calculate P_f which is given by

$$P_f = P(F_m) = P(F_1) \prod_{i=1}^{m-1} P(F_{i+1} | F_i), \quad (13)$$

where F_i represents intermediate failure event i . By making the conditional probability of samples falling in the intermediate failure regions large the variance of each individual failure event can be minimised, thereby minimising the variance of P_f . Markov chains are used to generate conditional samples from one failure region to the next in order to calculate $P(F_{i+1}|F_i)$. A complete description of the method is given in Au & Beck (2001).

RESULTS

The probability of failure for the system at design pressure is shown in Table 4. The probability of failure for the system at $P = 5.4 P_d$ is shown in Table 5.

Table 4: Probability of failure at $P = P_d$ computed by different methods.

Method	P_f	Variance of P_f
Advanced FORM	2.7×10^{-8}	Not Applicable
Subset Simulation	7.8×10^{-8}	2.4×10^{-9}
Importance Sampling	6.7×10^{-8}	1.8×10^{-9}

Table 5: Probability of failure at $P = 5.4P_d$ computed by different methods.

Method	P_f	Variance of P_f
Advanced FORM	0.507	Not Applicable
Monte Carlo	0.489	0.005

DISCUSSION

Although the advanced FORM result at the design pressure has slight disagreement with the Monte Carlo value of P_f , it is correct to an order of magnitude and therefore serves as a useful estimator for P_f . In addition, the percentage error of the FORM is reduced at higher values of P_f (for example, at $P = 5.4P_d$ the probability of failure computed by FORM is 0.51 and the value computed by Monte Carlo is 0.49), and therefore for most of the fragility curve the FORM gives a reasonably accurate approximation.

SENSITIVITY ANALYSIS

We would like to know which uncertainties make important contributions to our calculated measure of uncertainty, which in this case is the uncertainty in P_f . The uncertainty in P_f is caused by uncertainty in coefficients of variation of input parameters to the advanced FORM analysis. This type of sensitivity analysis, where parameters are ranked in order of their importance, is known as Factors Prioritisation (FP) (Saltelli, 2008).

A wide variety of methods exist for performing sensitivity analysis, and these methods fall into several broad categories. Sensitivity analysis methods can be local or global, by considering the sensitivity at just one point in the input space or many. In addition the methods can consider the sensitivity to variables on their own or to several variables at a time.

SOBOL INDICES

One frequently used method of sensitivity analysis is the so called Sobol indices or variance based sensitivity indices. The purpose of Sobol indices is to decompose the variance of the output into variances attributable to each input. Therefore, Sobol indices are a global method of sensitivity analysis. A derivation is available in Sobol (2001).

The Sobol indices are

$$S_i = \frac{V_{X_i} [E_{X_{\sim i}}(Y | X_i)]}{V(Y)} \quad (14)$$

for the single input X_i , where Y is the output of interest. V and E represent the variance and expected value, respectively. The total sensitivity indices are given by

$$T_i = 1 - \frac{V_{X_{\sim i}} [E_{X_i}(Y | X_{\sim i})]}{V(Y)} \quad (15)$$

which measures the effect of the variable X_i including all interactions. The Sobol and Total sensitivity indices can be computed by Monte Carlo simulation. In some cases, for example when the model has too many parameters or the model is very computationally expensive, it is necessary to use a more complex method to compute the Sobol and total sensitivity indices.

For example, the upper bound of the Total Sensitivity index can be efficiently calculated by integrating the local sensitivity analysis over the whole space of the inputs (Patelli et al, 2010), and the Sobol indices can be efficiently calculated by use of the FAST method given in Tarantola et al. (2006).

METHOD

The Sobol indices for the sensitivity of P_f , calculated by the advanced FORM method, with respect to the coefficients of variation of each parameter in Table 2 were calculated using OpenCOSSAN. A uniform distribution between 0 and 1 was applied for the coefficients of variation of the input parameters to the advanced FORM, i.e. any value for the coefficients of variation was equally likely, as this is a commonly used uninformative distribution. This assumption is somewhat unjustified as even if the coefficients of variation all fall within this interval there is no reason to assume that each value is equally likely in reality. However, in this case it is a useful approximation as it allows us to study the effect of an arbitrary variation in this parameter. The mean values for the parameters were taken from Table 2.

The analysis was then repeated with $P = 5.4P_d$ (chosen for the strength to design load ratio calculated in the previous section in order to make $P_f=0.5$) and $P = 5P_d$. At increased pressures the variance in the Sobol and Total Sensitivity indices computed by Monte Carlo simulation was impracticably high and so it was necessary to compute the Sobol indices using the FAST method (Tarantola et al, 2006) and the upper bound of the Total Sensitivity indices using Patelli's method (Patelli et al, 2010), both of which have been implemented in OpenCOSSAN. This allowed the calculation to be completed in a shorter time as fewer samples were required.

RESULTS

The calculated Sobol Indices and Total Effects Indices when $P = P_d$ are shown in a bar plot in Figure 7. It is clear that the biggest contributors to uncertainty in the output are the coefficients of variation of A_t and F_t . The bar plots show error bars to represent our uncertainty in the Monte Carlo estimators for the indices.

Figures 8 and 9 show the effect of varying A_t and F_t separately, whilst keeping the other variables fixed at their values from Table 2. There is a sharp increase in failure probability when the coefficient of variation is larger than 0.2. Further analysis shows that the location for this 'knee' in the graph depends upon the value of the other parameters, i.e. if the other coefficients of variation are set as 0.3 then the location of the knee changes to 0.3. Figure 10 shows the effect of varying both of these parameters simultaneously.

The calculated Sobol Indices and Total Effects Indices upper bounds for $P = 5.4P_d$ are shown in a bar plot in Figure 11. It is clear that the biggest contributors to uncertainty in the output are the coefficients of variation of R and P , followed by F_t and A_t . Figure 12 shows the effect of varying P and R simultaneously when $P = 5.4P_d$, whilst keeping the other variables fixed at their values from Table 2.

The calculated Sobol Indices and Total Effects Indices upper bounds for $P = 5P_d$ are shown in a bar plot in Figure 13. Again, it is clear that the biggest contributors to uncertainty in the output are the coefficients of variation of R and P , followed by F_t and A_t . Figure 14 shows the effect of varying P and R simultaneously when $P = 5P_d$, whilst keeping the other variables fixed at their values from Table 2.

DISCUSSION

The results show a large variability of the failure probability at the design pressure for changing coefficients of variation of A_t and F_t , and this could possibly be explained by the large mean value of these variables. At increased pressures it is clear that the coefficients of variation of P and R play a greater role in the variability of P_f .

It is interesting to note that the variability of P_f is greatly decreased when $P = 5.4P_d$, implying that the choice of coefficient of variation is unimportant when $P_f=0.5$, which justifies the use of the simplified method for when the applied pressure is equal to the strength. Intuitively it is clear that if a distribution is centred on the edge of the failure region (i.e. on the limit state function) then changing the coefficient of variation of the input variables should not significantly move the probability density from the safe region into the failure region.

There is significant variability of P_f when $P = 5P_d$, however the failure probability appears to plateau when the coefficients of variation of P and R are above approximately 0.5. This implies that if there is no data to determine of the Coefficient of Variation then a larger coefficient of variation would be a conservative choice for this pressure. In this context a conservative choice is one which gives an overestimate of P_f . An overestimate is preferable to an underestimate as implying a structure is safer than it is in reality could have severe consequences. However, we also wish for our estimates to be as close as possible to the true value of P_f as large overestimates can cause unnecessary over engineering which is undesirable as this can lead to increased costs. The size of coefficient for which this plateau takes place is dependent on mean applied pressure, and this should be considered when attempting to find a conservative value of the coefficients of variation. Moreover, for applied pressures above the strength Figure 14 shows that choosing a lower value of the coefficients of variation would be conservative in this case.

Our analysis appears to justify the choice of coefficients of variation chosen in this work, as the values given in Spencer et al. (2006) and Sundararajan (1995) are less than those chosen here, and hence the assumptions for these parameters in this paper can be considered conservative for applied pressures below the strength.

If engineering judgement can be used to justify the irrelevance of the tails of the fragility curve to the analysis being performed then the impact of using an approximate value of the Coefficient of Variation is lessened, however appropriate conservatism should still be applied.

In future calculations, in order to accurately describe our epistemic uncertainty in these parameters, particularly in the tails of the fragility curve, we should use a more considered approach to uncertainty where possible. For example if a more accurate estimation of the coefficient of variation cannot be obtained it may be necessary to construct a probability box by defining the coefficient of variation as an interval (Ferson, 2003). This approach can be understood as the engineer testing many different values for the coefficient of variation of each variable and choosing the most and least conservative values to give an interval for P_f (in practice the engineer would use a sophisticated optimisation algorithm coupled with conventional reliability analysis to perform the calculation).

If the coefficients of variation were assumed to be fuzzy variables it would be possible to determine the range of possible values of these coefficients which maintain an acceptably low P_f , with no requirement to repeat the analysis multiple times (Beer, 2011). This presents a significant computational benefit. The acceptable range for P_f would be specified by the engineer and could be taken from an appropriate design code. Such an approach is known as Factor Mapping (FM), and could be particularly useful for industrial design applications.

CONCLUSIONS

First Order Reliability Method (FORM) is applied to predict probability of failure of the containments. Probability of failure vs internal pressure is presented for both types of containments (with and without steel liner). Previous studies undertaken as part of the two international roundrobin exercises have established the ultimate structural collapse mode of the containments under internal pressure loading which indicates that the failure takes place in the general field of the containment wall around mid-height and away from any major structural discontinuities. This is because robust design procedures have been used that provide adequate compensation and local strengthening to avoid structural failure at discontinuities. Based on these experimental studies and the attendant numerical analyses a failure function is presented that assumes first yielding in the hoop direction at mid-height of the cylinder wall. It is shown that when the load term (given by $P \times \text{mid-radius of the wall}$) equalises the strength terms (given by $\text{crosssectional area/unit height} \times \text{yield stress}$) for rebar, liner, tendon and concrete then the probability of failure of structural collapse of the containment is 50%. The paper presents a simple method to establish structural reliability of a pre-stressed concrete containment which can be useful for probabilistic safety assessment when considering extreme events that lead to over-pressurisation of the containment.

It has been shown that there is a strong dependence of the probability of failure of a concrete containment computed by advanced FORM on the coefficients of variation of the Rebar Yield and Rebar Area at the design pressure. The coefficients of variation of the pressure and radius are also important parameters, especially in the centre of the fragility curve when the applied pressure is increased. The variability of the probability of failure is decreased at this applied pressure; however it is still important to apply conservatism in scenarios where we lack knowledge of the true value of these parameters. This illustrates the importance of ensuring that the choice of these parameters is justified by evidence from real models, as a failure to choose an appropriate value could result in an order of magnitude error on the probability of failure at the design pressure. However, less caution is required when we simply wish to find the pressure at which $P_f=0.5$.

REFERENCES

- Au, S.K. and Beck J.L. (2001). "Estimation of small failure probabilities in high dimensions by Subset Simulation". *Probabilistic Engineering Mechanics* 16.4: 263-277.
- Beer, M. et al. (2011). "Structural reliability assessment with fuzzy probabilities". *Proceeding of ISIPTA*.
- Ferson, Scott, et al. (2003). "Constructing probability boxes and Dempster-Shafer structures". *Sandia National Laboratories*: 143-180.
- Kamatam, K and Prinja N.K. (2011). "Analysis of the BARC Containment Model", *Transactions SMiRT* 21, New Delhi, India, Paper 820.
- Patelli, E, Pradlwarter, H.J. and Schuëller, G.I. (2010). "Global sensitivity of structural variability by random sampling". *Computer Physics Communications* 181.12: 2072-2081.
- Patelli, E. (2016). "COSSAN: A Multidisciplinary Software Suite for Uncertainty Quantification and Risk Management". *Handbook of Uncertainty Quantification*. Ed. by Roger Ghanem, David Higdon, and Houman Owhadi. Cham: Springer International Publishing, pp. 1–69.
- Patelli, E., et al. (2014). "OpenCossan: An efficient open tool for dealing with epistemic and aleatory uncertainties". *Vulnerability, Uncertainty, and Risk: Quantification, Mitigation, and Management*. ASCE.

Prinja, N.K. and Shepherd, D. (2003). “Numerical Simulation of Limit Load Testing of ¼ Scale Pre-stressed Concrete Containment Vessel, Pressure Equipment Technology - Theory and Practice”, Professional Engineering Publishing Limited.

Rackwitz, R. (1976). “Principles and methods for a practical probabilistic approach to structural safety”, Sub-committee for First Order Reliability Concepts for Design Codes of the Joint CEB-CECM-CIB-FIP-IABSE Committee on Structural Safety, CEB Bulletin N112.

Saltelli, A., et al. (2008). “Global sensitivity analysis: the primer”. John Wiley & Sons.

Schuëller, G.I, and Stix, R. (1987). “A critical appraisal of methods to determine failure probabilities”. Structural Safety 4.4: 293-309.

Sobol, I.M. (2001). “Global sensitivity indices for nonlinear mathematical models and their Monte Carlo estimates”. Mathematics and computers in simulation 55.1: 271-280.

Spencer, B. W., Petti, J. P. and Kunsman, D. M. (2006). “Risk-informed assessment of degraded containment vessels”. Sandia National Laboratories, Albuquerque, NM.

Sundararajan, C. R. (1995). ”Probabilistic structural mechanics handbook: theory and industrial applications”. Chapman & Hall.

Tarantola, S, Gatelli, D. and Mara, T.A. (2006). “Random balance designs for the estimation of first order global sensitivity indices”. Reliability Engineering & System Safety 91.6: 717-727.

ABBREVIATIONS

BARCOM	Bhabha Atomic Research Centre (BARC) Containment test model
CoV	Coefficient of Variation
FEA	Finite Element Analysis
FORM	First Order Reliability Method
PCCV	Pre-stressed Concrete Containment Vessel
SNL	Sandia National Laboratories

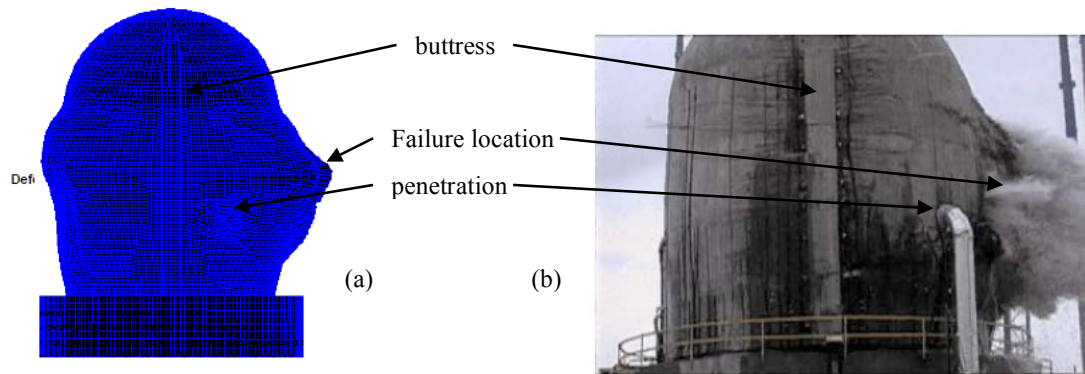


Figure 1. Predicted failure mode of the SNL model (a) FEA results vs (b) test at $P=3.65 \text{ Pd}$

(Figure in colour please)

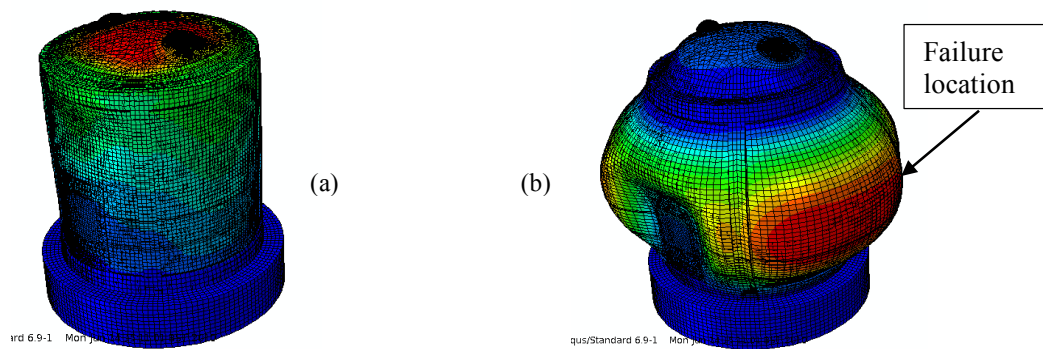


Figure 2. Predicted response of the BARC model (a) under prestress only and (b) at $P=2.89 \text{ Pd}$
(Figure in colour please)

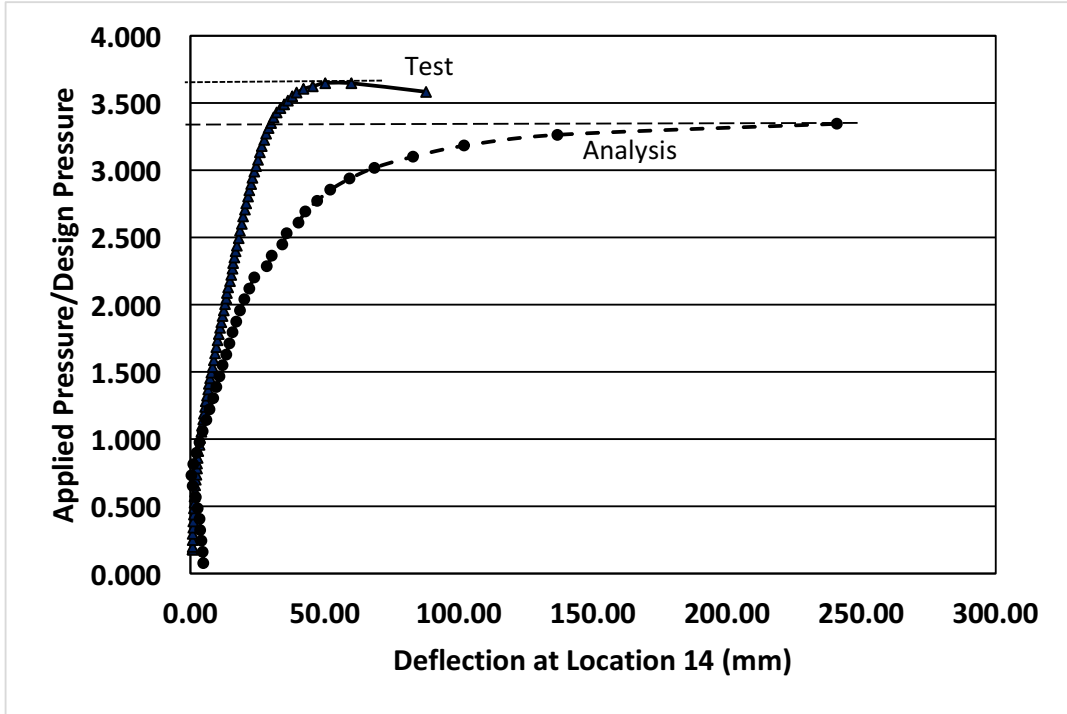


Figure 3. SNL test vs analysis comparison of deflection near failure location

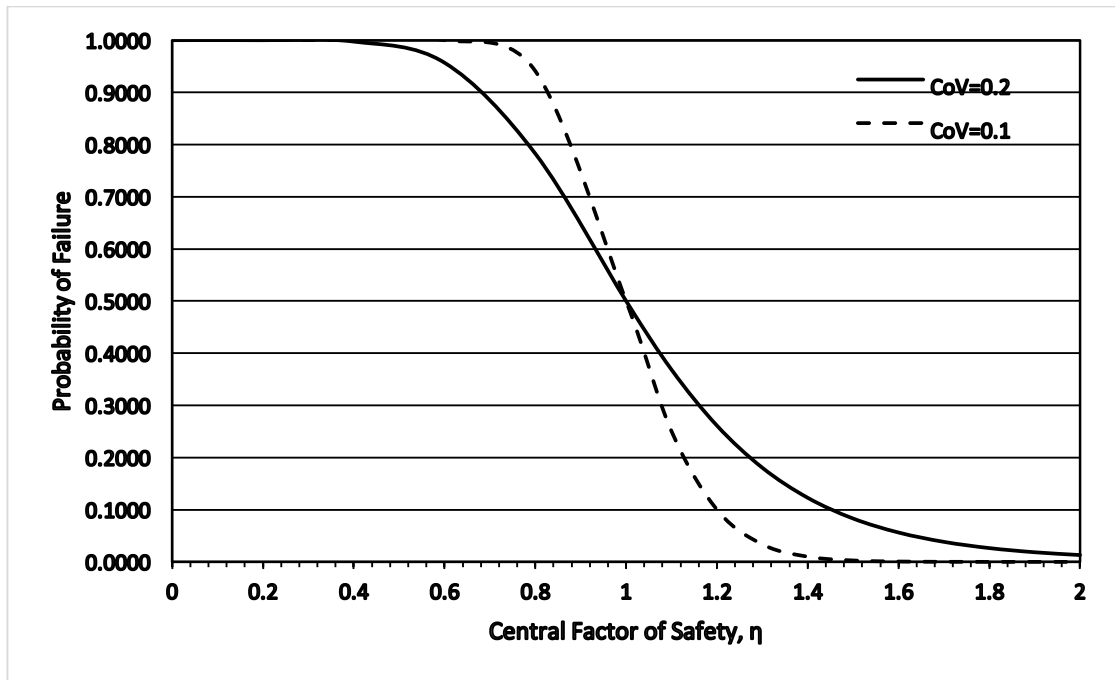


Figure 4. Probability of failure vs Central Factor of Safety

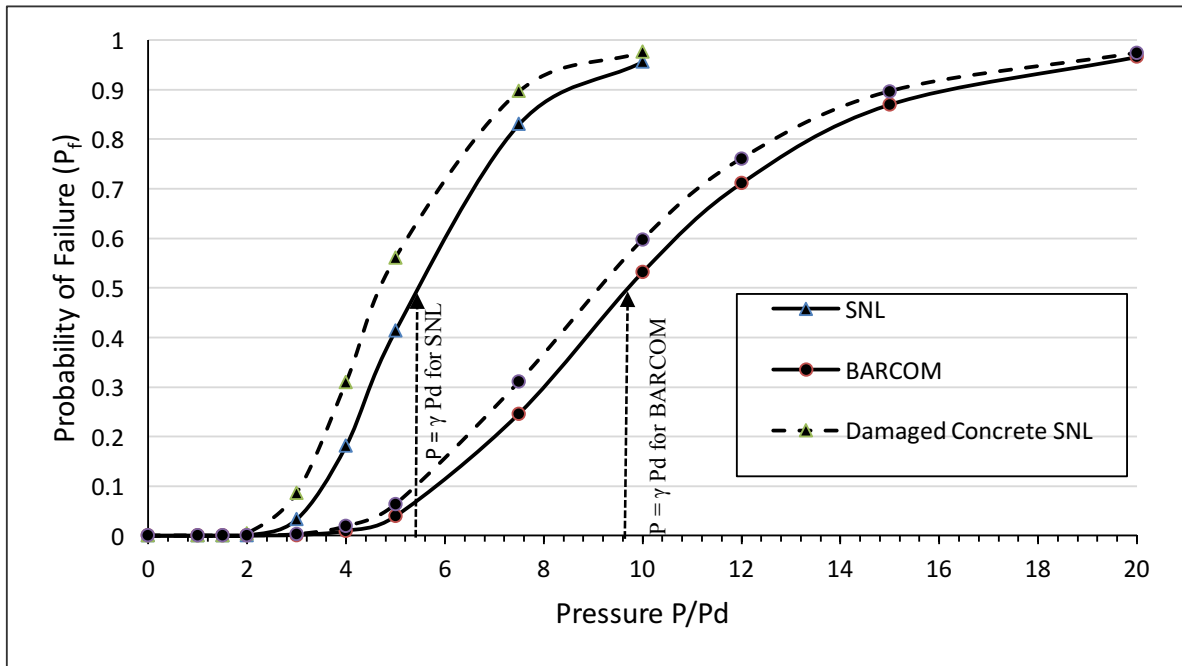


Figure 5. Containment P/P_d vs P_f

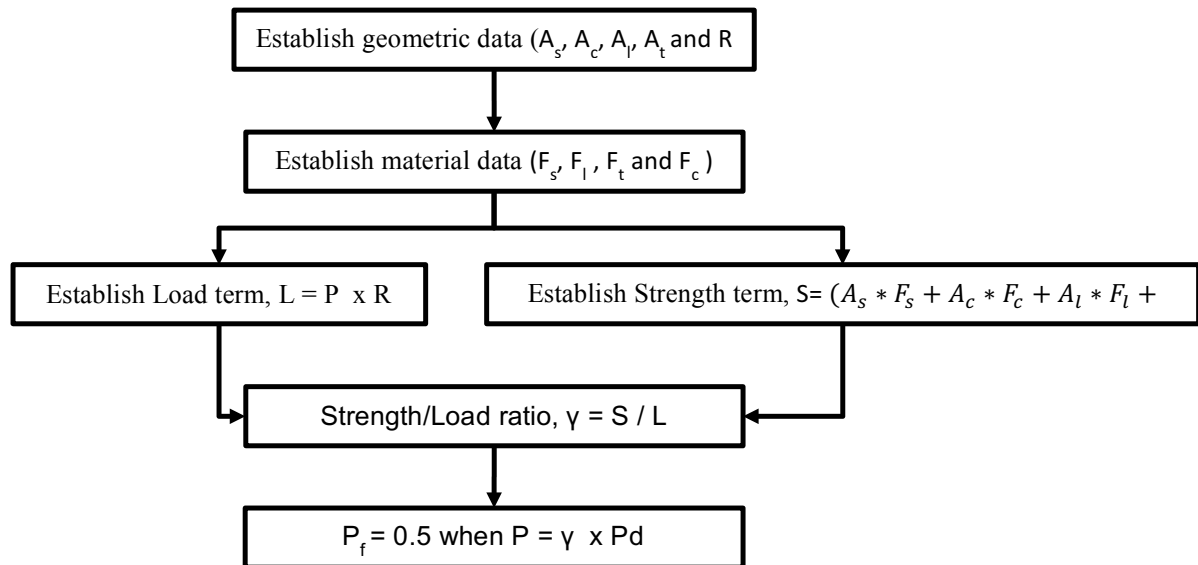


Figure 6. Simplified method to establish P_f of concrete containment

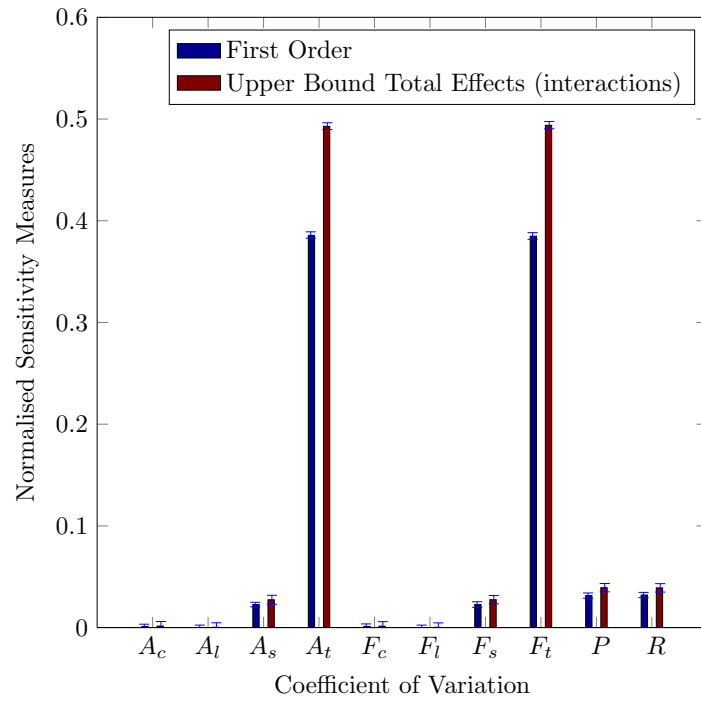


Figure 7. Plot of Sobol Indices and Total Sensitivity Indices for uncertain coefficient of variation for all input parameters to advanced FORM at $P = P_d$. The error bars represent one standard deviation.

(Figure in colour please)

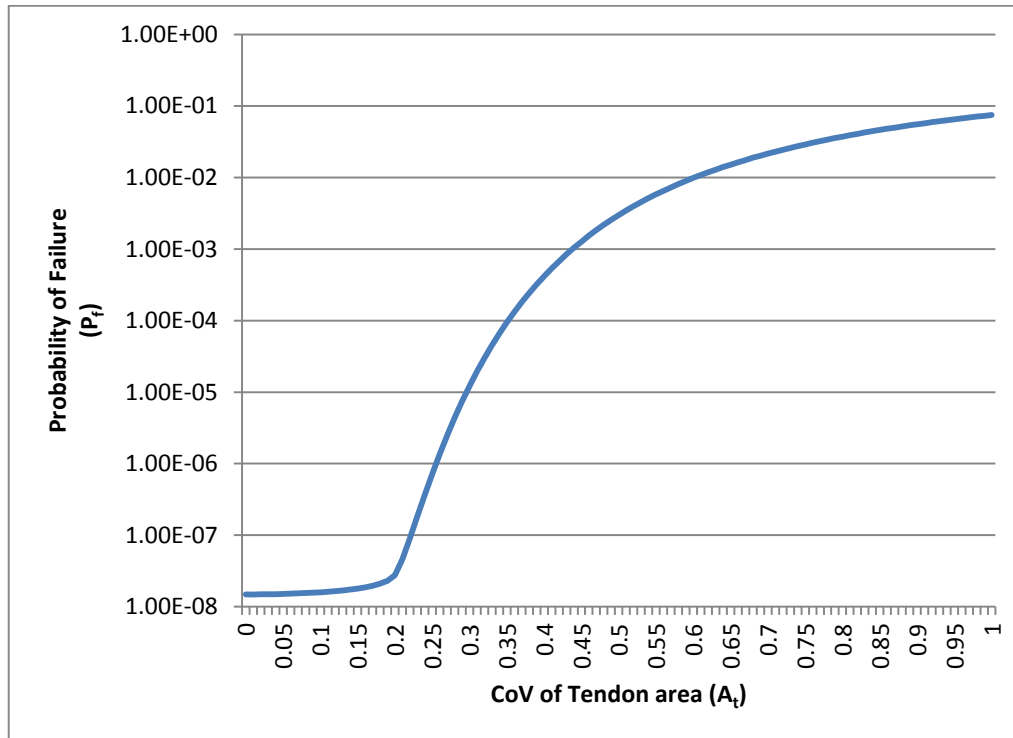


Figure 8. Plot of failure probability at $P = P_d$ for varying coefficient of variation of tendon area, A_t , while keeping other variables fixed.

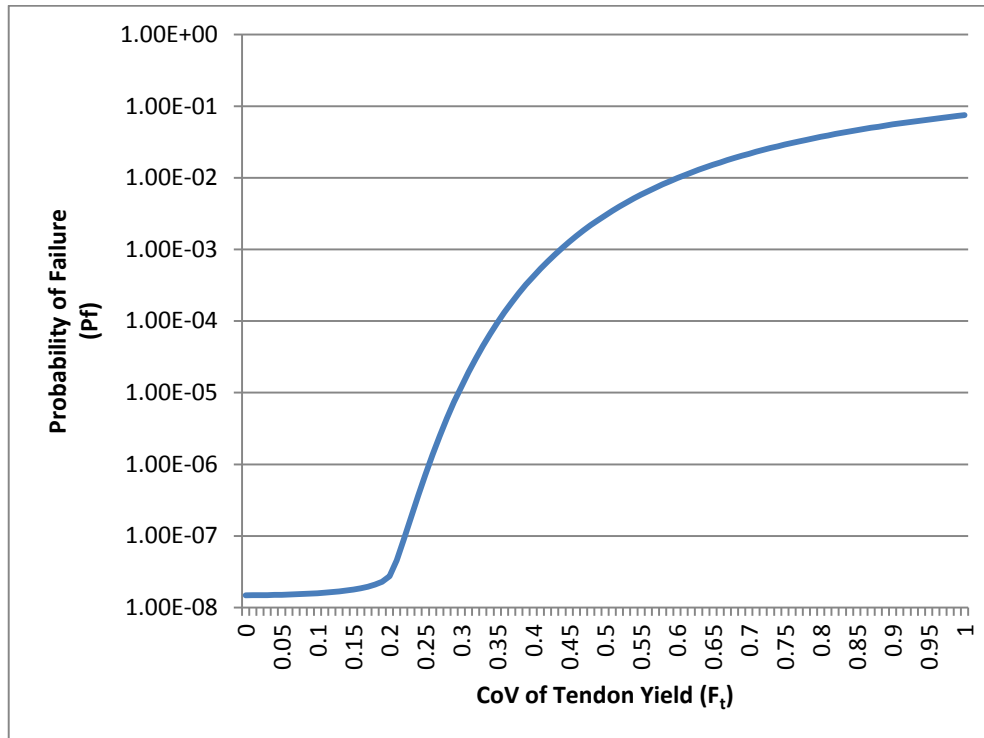


Figure 9. Plot of failure probability at $P = P_d$ for varying coefficient of variation of tendon yield, F_t , while keeping other variables fixed.

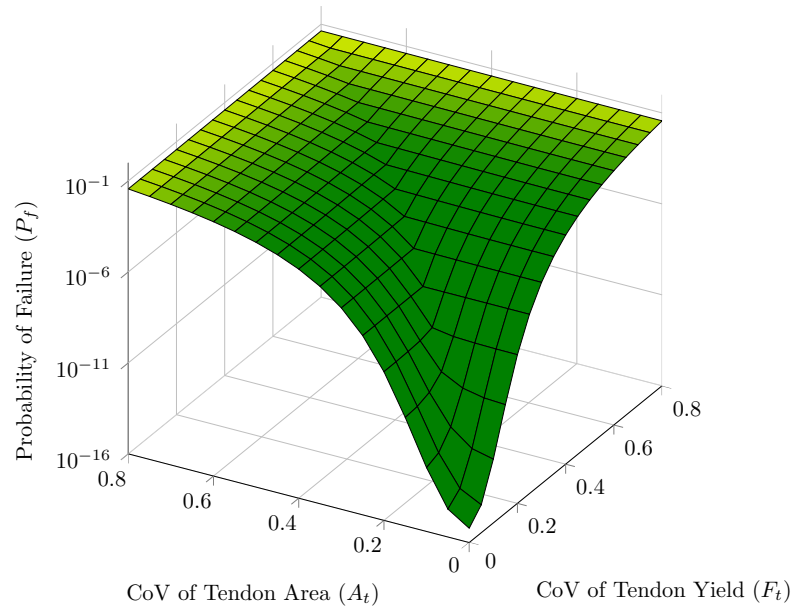


Figure 10. Plot of failure probability at $P = P_d$ for varying coefficient of variation of tendon yield, F_t , and tendon area, A_t , while keeping other variables fixed.

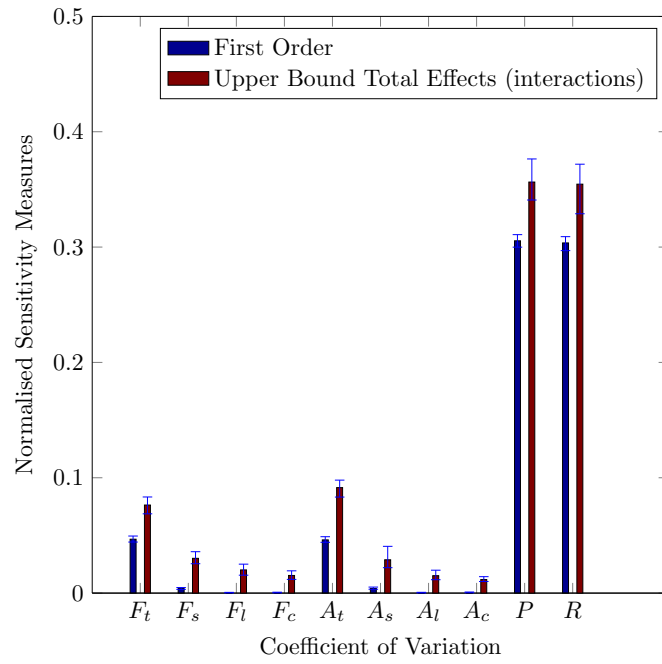
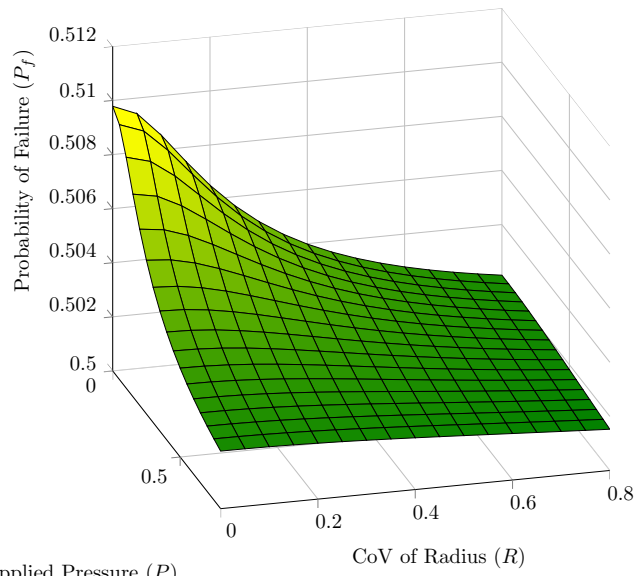


Figure 11. Plot of Sobol Indices and Total Sensitivity (upper bound) Indices for uncertain coefficient of variation for input parameters to advanced FORM at $P = 5.4P_d$. In this figure the error bars represent the 5%-95% confidence interval.



CoV of Applied Pressure (P)

CoV of Radius (R)

Figure 12. Plot of failure probability at $P = 5.4P_d$ for varying coefficient of variation of applied pressure, P , and radius, R , while keeping other variables fixed.

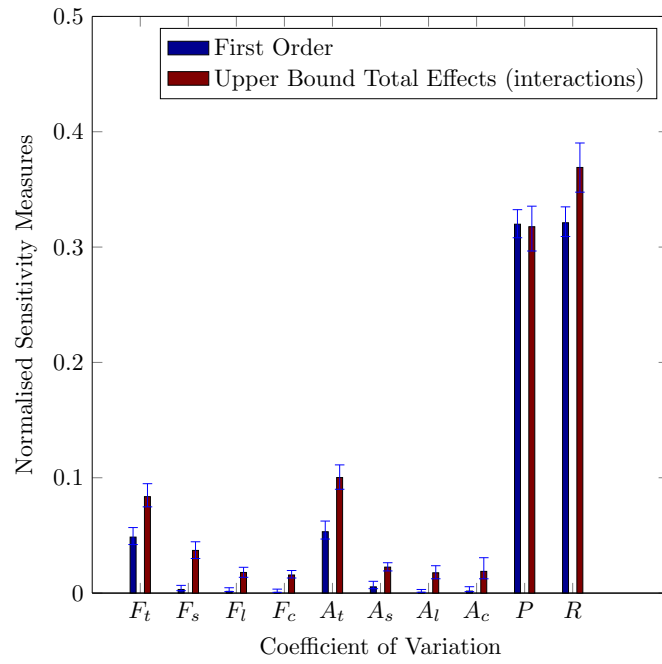


Figure 13. Plot of Sobol Indices and Total Sensitivity (upper bound) Indices for uncertain coefficient of variation for input parameters to advanced FORM at $P = 5P_d$. In this figure the error bars represent the 5%-95% confidence interval.

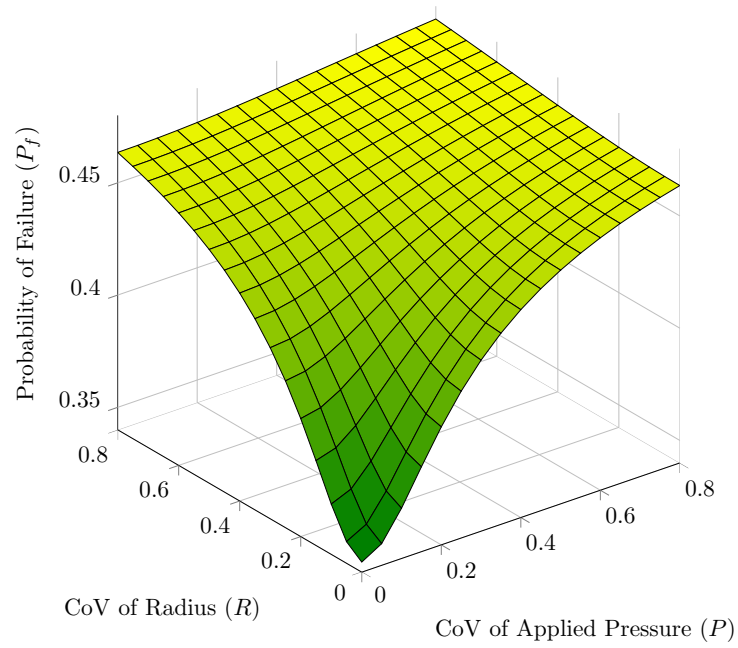


Figure 14. Plot of failure probability at $P = 5P_d$ for varying coefficient of variation of applied pressure, P , and radius, R , while keeping other variables fixed.